HYDROTHERMAL SYNTHESIS OF ZNO NANOSTRUCTURES FOR ROOM TEMPERATURE NO_2 GAS SENSING ANALYSIS

S. Roseline Mariyal[1], D. Benny Anburaj[2*], G. Nedunchezhian[3], S. Joshua Gnanamuthu[4]

Abstract:
A ZnO nanostructure was successfully synthesized via a facile and efficient hydrothermal method. The sample was characterized by XRD, SEM, UV-vis and Photoluminescence (PL) techniques. The XRD pattern revealed that the sample was well crystallized in a hexagonal wurtzite structure. SEM images showed that the as-prepared ZnO exhibited a rods like nanostructure, which was self-assembled by thin and uniform nanorods with a thickness of approximately 30 nm. UV-vis spectra showed that a significant blue-shift in the absorption edge for the as-prepared ZnO as compared to the commercial ZnO. PL spectra indicated that the concentration of surface oxygen vacancies in the as prepared ZnO was much higher than that of the commercial ZnO. Furthermore, the nanorod assembled ZnO nanostructure exhibited excellent gas sensing properties towards NO_2, indicating that the as-prepared ZnO architecture is a promising material for gas sensors.

Keywords: Hydrothermal synthesis, NO_2 sensing, ZnO, VOC

[1,2*]P.G and Research Department of Physics, D.G.Govt Arts College , Mayiladuthurai-609 001. (Affiliated to Bharathidasan University, Tiruchirappalli-24, Tamil Nadu,India)
[3]PG & Research Department of Physics, Thiru. Vi. Ka. Govt. Arts College, Thiruvarur-610003. (Affiliated to Bharathidasan University, Tiruchirappalli - 24,Tamil Nadu ,India)
[4]P.G and Research Department of Physics, TBML College, Porayar-609307. *(Affiliated to Bharathidasan University, Tiruchirappalli - 24,Tamil Nadu ,India)*

***Corresponding Author:** Dr.D.Benny Anburaj
*****P.G and Research Department of Physics, D.G.Govt Arts College , Mayiladuthurai-609 001. (Affiliated to Bharathidasan University, Tiruchirappalli-24, Tamil Nadu,India), bennyanburaj@rediffmail.com

DOI: - 10.48047/ecb/2023.12.si10.00218

1. Introduction

With the rapid development of industrialization and urbanization in the past few decades, environment pollution caused by the volatilization of hazardous gases has become an important issue. Environment pollution due to increase of greenhouse gases such as CO_2, CH_4, NO_2, CO, SO_2, and NH_3 in the atmosphere is a major problem in the world. The higher industrialization lead to the increased emission of toxic gases is one of the reasons of pollution. In addition, gases emitted by vehicles, burning of agriculture products, volcanic activity etc, are other reasons for environmental pollution. Metal-oxide semiconductor nonmaterial's has drawn extensive attention from researchers owing to their unique physicochemical properties and multifunctional applications [1-7].

Zinc oxide (ZnO), as an eminent n-type semiconductor with wide band gap of 3.37 eV and large exciton binding energy of 60 meV, which occupies an important position in various metal-oxide nanomaterials because of its preeminent electrical, optical and catalytic behaviours, has been widely utilized in gas sensors [8], solar cells, photocatalyst [9, 10] and etc.. In recent years, countless endeavours have been poured on the development of gas sensors based on nanostructured ZnO to achieve the effective detection of hazardous gases. As is known to all, the sensing mechanism of ZnO is primarily controlled by its surface [11]. Therefore, tailoring the structure and morphology of ZnO becomes the key to optimizing the gas-sensing performances [12]. It's well known that the properties of ZnO depend highly on its nanostructures, including crystal size, orientation and morphology. As a consequence, ZnO nanocrystals with highly controlled microstructures have been investigated extensively in recent years [13-15].

The nanosized ZnO offers outstanding gas sensitivity [16-17] and fine selectivity to various gases [18-19]. The gas sensing property of a material actually related to its morphology [20]. The high surface area is essential requirement for high response of gas sensors. Nanostructures with higher surface area with more adsorption sites are preferred structures for gas sensing applications. Porosity of ZnO nanostructures increases the surface area and number of active adsorption sites so is it can absorb the gas particles on the surface on nanotubes therefore, improves gas response. Hydrothermal technique has been used for preparation of nano structured materials with high controllability. The method is very simple, green, and low cost, has been used for synthesis of various morphologies of ZnO nanostructures successfully.

2. Experimental details

2.1Synthesis of ZnO nanoparticles

ZnO nano powder were synthesized by simple hydrothermal method using the aqueous solution of Zinc acetylacetonate hydrate (Zn $(acac)_2$) and NH_4OH. In a typical synthesis process 1.3631 g of (Zn $(acac)_2$) was dissolved in 100 ml of distilled water and NH_4OH was added drop by drop to maintain the pH of solution 7 under constant stirring. Then this solution was continuously stirred for 1 hour and the resultant solution was transferred to Teflon-lined stainless steel autoclave of 100 ml volume and maintained at 150 °C for 3 hours in muffle furnace. After the hydrothermal reaction the autoclave was naturally allowed to cool to room temperature. The product of white precipitate was obtained and washed with distilled water and ethanol several times and dried at hot air oven at 60 °C. The dried particles were annealed at 300 °C for 3 hours. Similarly ZnO nanoparticles were prepared by hydrothermal method keeping the above experimental condition the same but the annealing temperature of the prepared dried particles was varying 400°C, 500°C and 600°C. The prepared ZnO nanoparticles were characterized for their structural, optical, and morphological properties and sensing studies.

2.2Characterization

Synthesized ZnO nanoparticles crystalline nature was analyzed by X-ray diffraction technique (PANalytical's X'Pert Pro). Field Emission Scanning Electron Microscopy and Energy Dispersive X-ray Spectroscopy (FEI Quanta FEG200) were employed to analyze the surface morphology and elemental composition of synthesized samples. KEITHLEY - Gas Sensor Test System was used for gas sensing to find the response of the nanostructures.

2.3Fabrication of gas sensing mechanism

The interaction mechanism between the analyte gas and the sensing material mainly involves fabricating a gas sensor. Substance like paste has been made by mixing ZnO NPs with isopropyl alcohol. A widespread layer was formed by coating the paste on the surface of the glass plate; in which two electrodes have been attached at each end of the sensing layer coated glass plate with the operating voltage of 10 volt. The entire gas sensing process was carried out in a closed

glass chamber of 1 liter which is placed on a magnetic stirrer and moderately heated using hot plate for vaporizing the liquefied as shown in Fig.1 analytes. When liquefied volatile organic reducing analyte like ammonia, acetone, ethanol, formaldehyde were injected in to the chamber using micropipette, it swiftly turned in to vapour state and made a contact with the sample. Larger the surface area of the sensing layer hence higher the sensitivity. The variation of electrical current of the sample owing to the exposure of target gas is measured by high efficient electrometer (Keithley 6517B, USA) controlled by a personal computer. Generally Sensing response was calculated by the formula $S = \frac{R_a}{R_g}$ (R_a>>R_g) for reducing gases, where R_a and R_g are the resistances of the sample in dry air and target gas.

In order to find the high selective behavior of the sensor the similar procedure is repeated for different samples of ZnO towards the various injected analytes at 200 ppm. Finally, one among the best sensor-analyte combinations is investigated for further gas sensing studies.

3. Results and discussion

3.1XRD Analysis

X-ray diffraction (XRD) pattern of synthesized ZnO nanoparticles are shown in Fig. 2 which confirm the formation of ZnO wurtzite (hexagonal) structure when compared with the corresponding peaks of JCPDS card no. 70-2205. One can observed that the intensity of the XRD peaks of ZnO particles prepared samples is relatively high. Further the intensity of XRD peak of (101) plane is relatively stronger in all the samples. The average crystallite size (D) of the synthesized ZnO nanoparticles was calculated from Debye-Scherrer formula from (101) plane.

$$D = K\lambda/\beta cos\theta$$

Interplanar distance (d) was calculated from Bragg's equitation

$$2dsin\theta = n\lambda$$

where θ is the angle of diffraction in degree, n=1 and λ is wavelength of X-rays used (1.5406 Å). Lattice cell parameters a (=b) $A = \pi r^2$and c were calculated from the relation of

$$\frac{1}{d^2} = \{\frac{4}{3}(\frac{h^2 + hk + a^2}{a^2}) + \frac{l^2}{c^2}\}$$

Where d is the interplanar distance and h, k and l are Miller indices of the plane. Average crystallite size of (101) plane is decreased from 46.01 nm to 33.85, 31.98 and 31.10 nm with increase in annealed temperature from 300°C,400°C, 500°C and 600°C respectively.

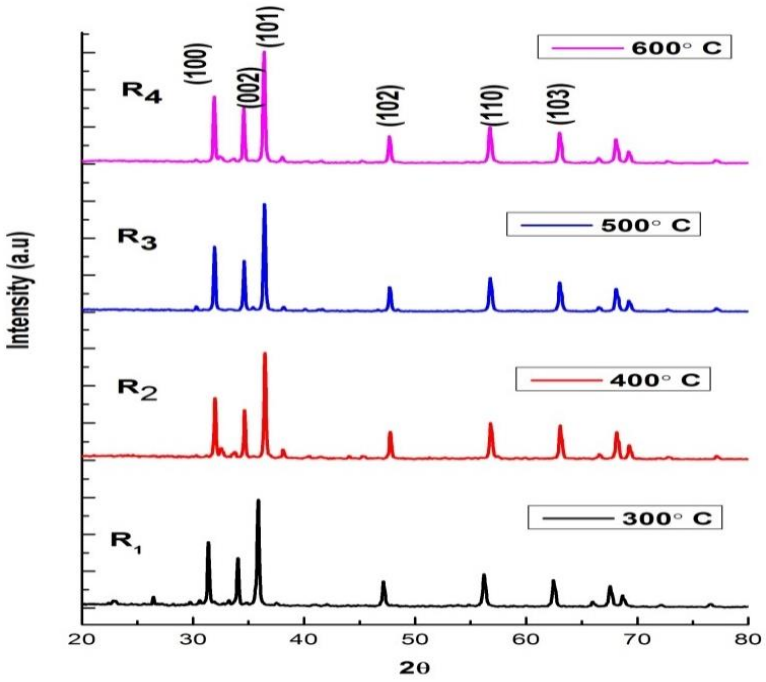

Fig 1 XRD patterns of synthesized ZnO NPs

Table 1. The average crystallite size and cell parameters of ZnO NPs

Temp ^{0}C	101 Plane			Cell Parameters (Å)	
	2θ degree	Average crystallite size D (nm)	Inter planner distance d (nm)	a=b	C
300	36.26	46.0	2.476	3.2521	5.2080
400	36.26	33.8	2.476	3.2513	5.2065
500	36.35	31.1	2.470	3.2403	5.1963
600	36.36	31.9	2.471	3.2423	5.1963

3.2. SEM and EDAX analysis

Details on the growth factors controlling the shape and size of ZnO nanostructures are presented in Fig.3 which shows the various morphology and shape selective synthesis of ZnO such as spindle like structure, hexagonal disks, spheroidal structures and elongated porous hexagonal nanorods structure. All the Figures (S1-S4) shows the uniform growth of ZnO nanostructures into high density flower like architectures composed of nanorods. Figure S1 shows the formation of aggregated ZnO nuclei in an initial homogeneous nucleation process. That nucleation was taking place to result in the formation of rod-like microstructures or amorphous precipitates, which are depicted in Fig. The SEM images of the ZnO nanorods are shown in S2 where one can indeed see many uniformly distributed rod-like nanostructures. Figure S3 shows the each grain of the initial ZnO nanostructures could grow primarily along one growth direction, the whole structure is made from a dozen of ZnO nanorods with a smooth surface and diameters of these nanorods and their length is up to several micrometers. Such a distinctive nanorod-like structure has many petals and pores, which are going to play a significant role in improving the gas sensing properties. Figure S4 shows the crystal surfaces containing defects tend to further decrease their energy through surface reconstruction, which provides active sites for secondary nucleation. Energy dispersive X-ray analysis (EDAX) spectrum of the prepared nanoparticle at S1, S2, S3 and S4 is shown in Fig. 4a-d respectively which reveals the presence of Zn and O. The absence of other elements other than 'Zn' and 'O' also confirms that the as formed product is pure.

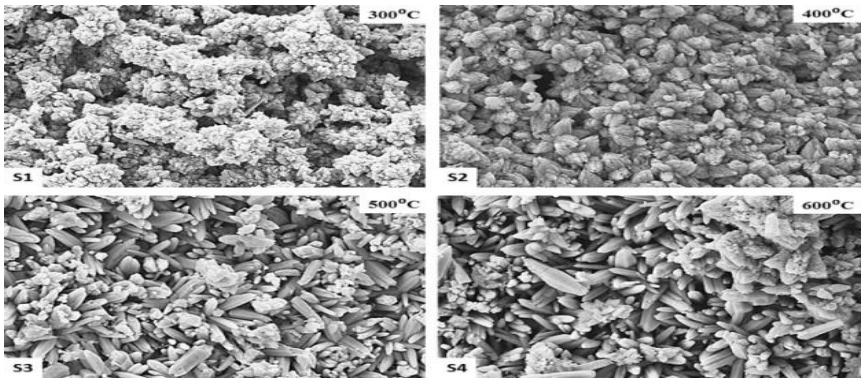

Fig. 2 SEM Analysis of Synthesized ZnO NPS

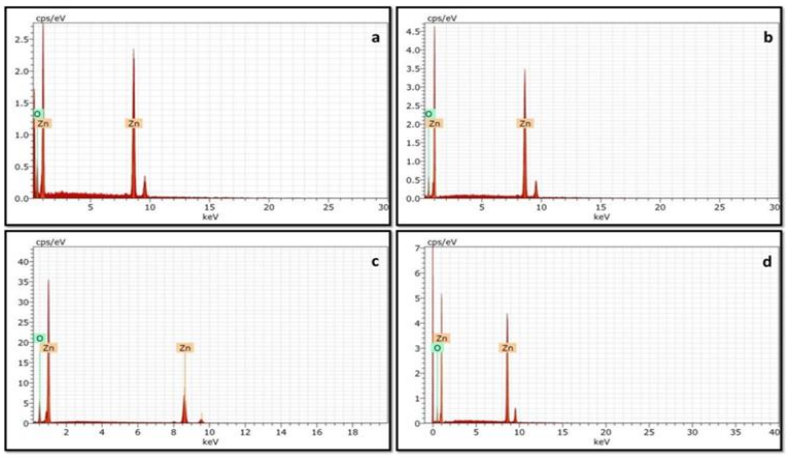

Fig. 3 EDAX Analysis of Synthesized ZnO NPS

3.3 PL Study

The gas-sensing mechanism of ZnO is the surface-controlled type, suggesting that gas response mainly depends on amount of defect, crystallinity and particle size of ZnO nanoparticles. Usually, the PL spectra are used to analyse the defects of semiconductor materials. Here, **Fig.7** shows the room-temperature PL spectrum of ZnO nanoparticles annealed at four temperatures with the excited wavelength of 349 nm. The PL spectrum of ZnO nanoparticles includes UV emission and visible emission. All the samples show a relatively strong UV emission peak, which results from the radiative recombination of an excited electron in the conduction band (e_{CB}^-) with the valence band hole (h_{VB}^+) . The defect-related visible emission is also detected, which is caused by the trapping of the electron - hole pairs by the defects and/or the surface states of the materials. The intensity of visible emission is directly related to the concentration of defects in the ZnO nanoparticles

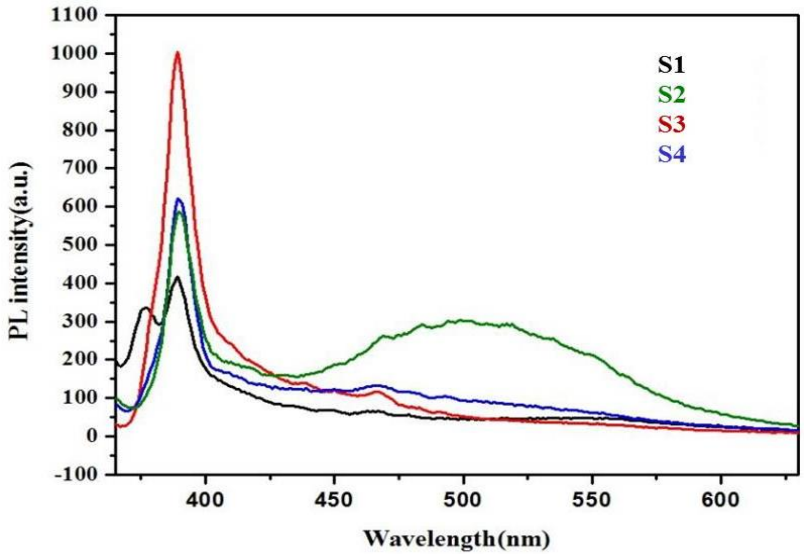

Fig. 4 PL Analysis of Synthesized ZnO NPS

3.4 Effects of Calcinations and Operation Temperatures on the Gas Sensitivities.

The ZnO nanorods prepared by calcining the ZnO sample at 300, 400, 500, and 600 ºC were denoted as S1, S2, S3, and S4 respectively. Nitrogen dioxide, a major poisonous gas in vehicle exhaust and chemical industry, was selected for evaluating the sensing property of the ZnO nanorods. The gas sensitivities of the ZnO nanorod sensors to 1.0 ppm NO_2 are listed in Figure 3. It is evident that S3 has the highest sensitivities at the operating temperature from 120 to 230 ºC. To investigate the difference of the sensing performances resulting from the calcinations temperatures, further characterizations were carried out.

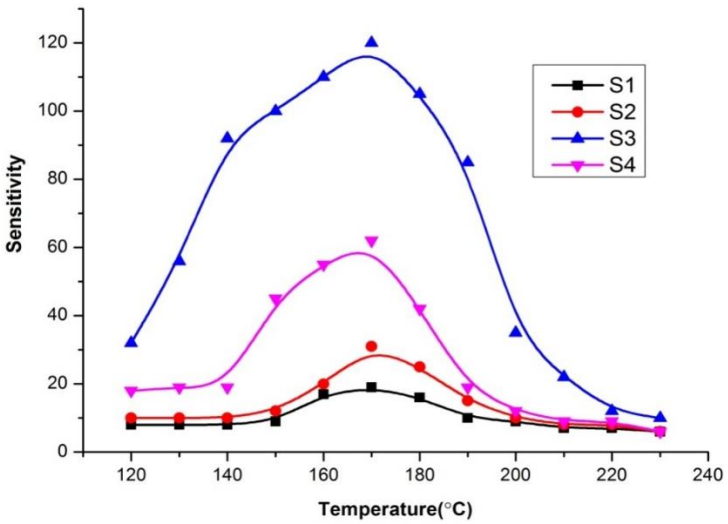

Fig. 5 Gas sensing Analysis of Synthesized ZnO NPS

3.5 Gas-sensing analysis

Sensing mechanism

The gas sensing mechanism of semi conducting metal oxide nano structures obviously rely on surface phenomenon. In general, the electrical conductivity of n-type semiconductor based metal oxide gas sensors be decided by the number of free electrons and usually contain oxygen deficiency.When ZnO is placed in clean air surrounded by its vicinity, the oxygen present in the air interacts with the surface and chemisorbed as O_2^-on the surface of the sensing material, there by capturing the electrons from the conduction band of ZnO, which causes lowering the number of free electrons in it, and reduces its conductivity by increasing the resistance of the sensing material itself. It causes further increment in the surface resistance and this value could be fixed as the baseline resistance (Ra). This occurrence mainly would develop a depletion region between the grain boundaries of the sample.

While sensing material is exposed under the influence of reducing gas like NO_2, which interacts with adsorbed oxygen, causing disengage the electrons from the control of adsorbed oxygen species. Those released electrons have retained in the conduction band of the sensing material.As the width of the space charge region was decreased and leads to a decrease insurface resistance thereby attaining the steady state NO_2 resistance (Rg).

3.6. Gas-sensing properties measurement of ZnO nanoparticles

Fig. 5 shows the gas response of ZnO nanoparticles to 50 ppm NO_2 as a function of operating temperature from 120 ºC to 230 ºC. For all the samples, the response to NO_2 is volcano type with increase in the operating temperature. Increase of operating temperature to a certain extent favors to improve amount of NO_2 chemisorptions, reaction rate occurring on the ZnO surface and conductivity behavior of ZnO nanoparticles, which enhances the gas response of ZnO nanoparticles. All the samples exhibit the maximum response to NO_2 at170 °C. When the operating temperature is beyond 170 °C, the gas response to NO_2 is reduced due to decrease of the amount of NO_2 adsorbed on ZnO surface. Furthermore, S3 has the highest response value to NO_2 among the investigated samples.

Besides, we further examined other gas-sensing properties of the S3 such as response time, recovery time and selectivity, which are important parameters for the gas sensor. Here, the response time is defined as the time for the sensor reaching 90% of its saturation value after the sensors are exposed to detected gases, and the recovery time is the time for recovery of the resistance to 90% of the initial level after exposing to air. The response time of the S_3 is less than 20 s, and the recovery time is 90 s, respectively. The study about long terms stability of this sensor is still in process, we will continue examine it.

Fig. 6 shows the selectivity of the ZnO sensors based on S3 sample to NO_2 relative to CO, NH_3 and CH_4 in the same gas concentrations. The gas sensing response to NO_2 is much higher than amount of NO_2 adsorbed on ZnO surface. Furthermore, S_3 has the highest response value to NO_2 among the investigated samples. for CO, NH_3 and CH_4 at each operating temperature in the range 120 – 230ºC, suggesting that the obtained S_3 nanoparticles have high selectivity

.

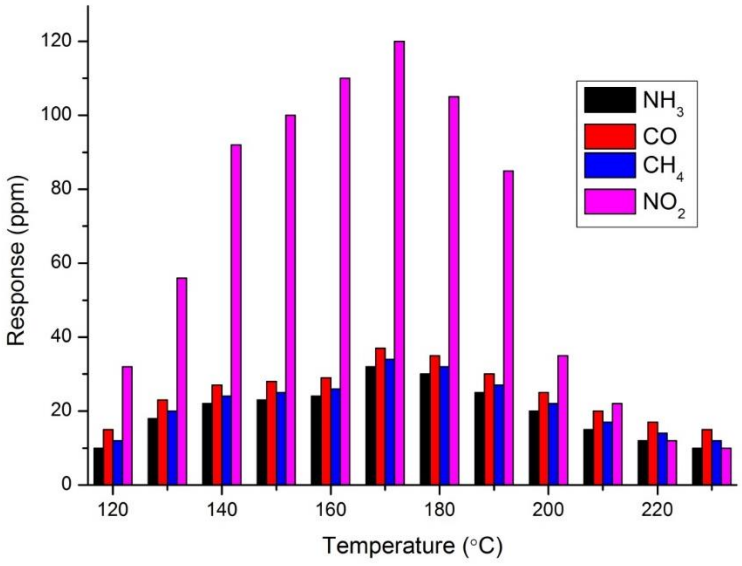

Fig. 6 Selectivity of ZnO sensors with gas sensing response

4. Conclusion

In summary, based on a facile, environment-friendly hydrothermal method, a three-dimensional (3D) rod like hierarchical ZnO nanostructure was successfully synthesized. The as-prepared ZnO is nanorod-assembled well-defined microstructure. while the thickness of each nanorods was about 30 nm. The possible formation mechanism was described as nucleation, growth and self-assembly of nanorods. The XRD result shows that the sample is well crystallized in a hexagonal wurtzite structure. Raman spectra exhibit that the sample keeps the crystal structure of the bulk ZnO and possesses more surface defects. UV-vis spectra show that a significant blue-shift in the absorption edge for the as-prepared ZnO as compared to commercial ZnO, which may be ascribed to the better crystallinity of the as-prepared ZnO. PL spectra indicate that the concentration of surface oxygen vacancies in the as prepared ZnO is much higher than that in the commercial ZnO. The gas sensing measurement indicates that the as-prepared ZnO exhibited excellent gas sensing properties towards NO_2. The enhanced NO_2 gas sensing properties of the present ZnO nanostructure can be attributed to the crystallinity, surface defects, unique structure, and nano junctions between adjacent nanorods. The facile synthesis of the present ZnO nanostructure together with its superior gas sensing performance provides a potentially new approach for the design and construction of ZnO-based sensor.

References

1. Y. Zhang, W. Zeng, New insight into gas sensing performance of nano needle-assembled and nanosheet-assembled hierarchical NiO nanoflowers, Mater. Lett., (2017) ,195, 217-219. doi.org/10.1016/j.matlet.2017.02.124
2. T. Li, W. Zeng, New insight into the gas sensing performance of SnO2 nanorod-assembled urchins based on their assembly density, Ceram. Int. 43 (2017) 728-735. DOI10.1016/j.ceramint.2016.10.001
3. R. Kumar, A. Umar, G. Kumar, H.S. Nalwa, A. Kumar, M.S. Akhtar, Zinc oxide nanostructure-based dye-sensitized solar cells, J.Mate. Sci. 52 (2017) 4743-4795. DOI:10.1007/s10853-016-0668-z
4. T. Li, M. He, W. Zeng, Polyhedral Cu2O crystal: Morphology evolution from meshed nanocube to solid and gas-sensing performance, J. Alloy. Compd. 712 (2017) 50-58. DOI10.1016/j.jallcom.2017.04.057
5. L. Zhu, W. Zeng, A novel coral rock-like ZnO and its gas sensing, Mater. Lett., 209 (2017) 244-246. doi: 10.1016/j.matlet.2017.08.020.
6. T. Zhou, P. Lu, Z. Zhang, Q. Wang, A. Umar, Perforated Co3O4 nanoneedles assembled in chrysanthemum-like Co3O4 structures for ultra-high sensitive hydrazine chemical sensor, Sens. Actuators B: Chem. 235 (2016) 457-465. https://doi.org/10.1016/j.snb.2016.05.075
7. L. Zhu, Y. Li, W. Zeng, UV enhanced enthanol sensor based on nanorod-assembled like ZnO, Physica E. 94 (2017) 123-125. doi:10.1016/j.physe.2017.08.004
8. Y. Al-Hadeethi, A. Umar, S.H. Al-Heniti, R. Kumar, S.H. Kim, X. Zhang, B.M. Raffah, 2D Sn-doped ZnO ultrathin nanosheet networks for enhanced acetone gas sensing application, Ceram. Int. 43 (2017) 2418-2423. DOI:10.1016/j.ceramint.2016.11.031
9. S. Singh, V.C. Srivastava, S.L. Lo, T.K. Mandal, G. Naresh, Morphology-controlled green approach for synthesizing the hierarchical self-assembled 3D porous ZnO superstructure with excellent catalytic activity, Micropor. Mesopor. Mater. 239 (2016) 296-309. DOI:10.1016/j.micromeso.2016.10.016
10. X. Chen, Z. Wu, D. Liu, Z. Gao, Preparation of ZnO photocatalyst for the efficient and rapid photocatalytic degradation of azo dyes, Nanoscale Res. Lett. 12 (2017) 143. doi.org/10.1186/s11671-017-1904-4
11. D.E. Motaung, G.H. Mhlongo, A.S. Bolokang, B.P. Dhonge, H.C. Swart, S. Sinha Ray, Improved sensitivity and selectivity of pristine zinc oxide nanostructures to H2S gas: Detailed study on the synthesis reaction time, Appl. Surf. Sci. 386 (2016) 210-223. DOI:10.1016/j.apsusc.2016.06.014
12. Huang JR, Shi CC, Fu GJ, Sun PP, Wang XY, Gu CP. Heteroatom-doped graphene materials: syntheses, properties and applications. *Mater Chem Phys*, 144, (2014), 34-38. doi.org/10.1039/C4CS00141A
13. Liu Y, Dong J, Hesketh PJ, Liu MLJ. The oxford handbook of nanoscience and technology. *Mater Chem*,15, (2005), 2316–2320.
14. Chen XS, Liu JY, Jing XY, Wang J, Song DL, Liu LH. A Review of One dimensional TiO2 Nanostructured Materials for Environmental and Energy Applications. *Mater Lett*, 112, (2013), 23–5.
15. Shao CJ, Chang YQ, Long Y. Sensors and Actuators B: Chemical. *Sens Actuator B Chem*, 204, (2014), 666–672.

16. Rai P, Kwak WK, Yu YT. Confined Formation of Ultrathin ZnO Nanorods/ Reduced Graphene Oxide Mesoporous Nanocomposites for High-Performance Room-Temperature NO2 Sensors. *ACS Appl Mater Interface*, 5, (2013), 3026–3032.
17. Wei SH, Wang SM, Zhang Y, Zhou MH. Gold Nanoparticles in Chemical and Biological Sensing *Sens Actuator B-Chem*, 192, (2014), 480–487.
18. Dem'yanets LN, Lyutin VI. Status of hydrothermal growth of bulk ZnO: Latest issues and advantages. *J Cryst Growth*, 310, (2008), 993–999. DOI:10.1016/j.jcrysgro.2007.11.145
19. Zhang Y, Liu TM, Lin LY, Hussain S, Wu SF, Zeng W, et al. Applications of graphene and related nanomaterials in analytical chemistry. *J Mater Sci-Mater Electron*,25, (2014), 376–381.
20. Y. Vijayakumar, G.K. Mani, M.V.R. Reddy, J.B.B. Rayappan, Nanostructured flower like V2O5 thin films and its room temperature sensing characteristics, *Ceram. Int*. 41, 2015, 2221–2227.